

Coherent Cooper-pair pumping by magnetic flux control

S. Gasparinetti

Low Temperature Laboratory (OVLL), Aalto University, P.O. Box 15100, FI-00076 Aalto, Finland

I. Kamleitner

Institut für Theory der Kondensierten Materie, Karlsruher Institut für Technologie, 76128 Karlsruhe, Germany

We introduce and discuss a scheme for Cooper-pair pumping. The scheme relies on the coherent transfer of a superposition of charge states across a superconducting island and is realized by adiabatic manipulation of magnetic fluxes. Differently from previous implementations, it does not require any modulation of electrostatic potentials. We find a peculiar dependence of the pumped charge on the superconducting phase bias across the pump and that an arbitrarily large amount of charge can be pumped in a single cycle when the phase bias is π . We explain these features and their relation to the adiabatic theorem.

PACS numbers: 85.25.Cp, 03.65.Vf, 03.65.Yz

I. INTRODUCTION

A Cooper-pair pump¹ is a superconducting device that can be used to transport Cooper pairs by manipulating some of its parameters in a periodic fashion. Cooper-pair pumping has recently attracted considerable theoretical^{1–14} and experimental^{15–19} attention.

Part of this attention stems from the geometric properties of the parametric cycle used to perform pumping. These properties, in turn, leave a distinctive fingerprint in the pumped charge. The link between geometric phases and pumped charge has been established in the adiabatic limit, where an explicit relation connects the pumped charge to the Berry phase^{20,21}, as first shown in Ref. 3 and experimentally demonstrated in Ref. 17. In addition, the breakdown of the adiabatic theorem caused by Landau-Zener transitions can be detected as a decrease in the pumped charge¹⁹. This offers the opportunity to develop Landau-Zener-Stückelberg interferometry based on geometric phases¹². Finally, it has been proposed to exploit Cooper-pair pumps for the observation of nonabelian geometric phases^{10,11}.

Another reason to study Cooper-pair pumps is that they are convenient solid-state implementations of a driven quantum two-level system. In the presence of a dissipative environment, the pumped charge is determined by the quasistationary state reached by the system and thus is a sensitive probe of decoherence effects. This explains why a Cooper-pair pump was chosen as a “case in point” in several theoretical works aimed at studying the role of dissipation in driven quantum systems, especially in association with the breakdown of the adiabatic theorem^{13,22–24}.

Different types of Cooper-pair pumps have been proposed and realized^{15,16,18}. All these devices comprise the same building blocks, namely, superconducting islands connected to each other and to superconducting leads by Josephson junctions. They are intended to be operated in a regime where the charging energy of the islands is much larger than the Josephson energies of the cou-

plings. Thus, at the heart of these implementations is the “classical” phenomenon of Coulomb blockade. Pumping relies on periodic modulation of electrostatic potentials, tuned by gate electrodes which act as pistons in pulling Cooper pairs onto and off the islands. As a result, the system spends most of its time in a state where Cooper pairs are localized, except for the short time required for their tunnelling between adjacent islands. The fact that a Cooper-pair can be delocalized between, say, an island and a lead, is of little relevance for a conventional Cooper-pair pump.

In this Article, we undertake a different approach to Cooper-pair pumping, that we call “flux pumping”. It is based on the adiabatic, coherent transfer of a superposition of charge states across a superconducting island, realized by magnetic flux control. In contrast to previous implementations, no modulation of electrostatic potentials is required. The device we consider uses the same hardware as the Cooper pair sluice introduced in Ref. 4 yet pumping is achieved in a completely different manner. The dependence of the pumped charge on the phase bias across the pump reveals unprecedented features. Among them, we find that for a particular choice of the system parameters, an arbitrarily large charge can be pumped per cycle. However, this is by no means inconsistent as at the same time the adiabaticity criterion requires the pumping cycle to be correspondingly slow.

The outline of this paper is as follows. In Sec. II, we introduce the Cooper-pair sluice and set up the theoretical framework on which our calculations are based. In the core Sec. III, we describe flux pumping. In Sec. IV, we characterize the breakdown of the adiabatic limit by performing numerical simulations with a Master-Equation approach. Finally, in Sec. V, we summarize our results and comment on the feasibility of our proposal.

II. THE COOPER-PAIR SLUICE

A schematic drawing of the Cooper-pair sluice is shown in Fig. 1 (a). It is a fully tunable Cooper-pair transistor,

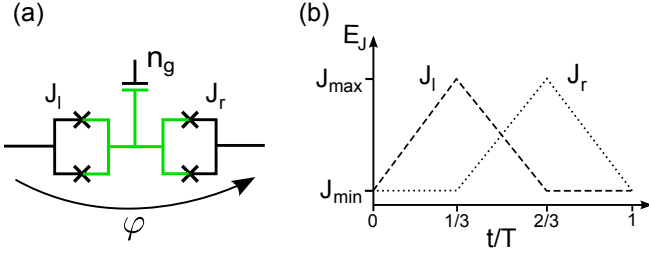


FIG. 1. (Color online) Pumping with magnetic fluxes. (a) Schematic circuit of a Cooper pair sluice. A superconducting island (green) is coupled to superconducting leads by two SQUIDs, acting as tunable Josephson junctions of energy J_l , J_r . A gate capacitively coupled to the island controls its polarization charge n_g . The superconducting phase of the two leads is held at a fixed difference φ . (b) Representative time modulation of J_l , J_r leading to flux pumping. The gate position is kept fixed throughout the modulation.

consisting of a small superconducting island connected to leads by two superconducting quantum interference devices (SQUIDs). The SQUIDs are controlled independently by adjusting the magnetic fluxes threaded by their loops, so that they can serve as Josephson junctions of tunable energy J_l , J_r . A gate electrode capacitively coupled to the island controls its polarization charge n_g . We will assume a constant superconducting phase difference φ across the device. This can be achieved, e.g., by shunting the sluice with a large Josephson junction¹⁷.

We use the sluice in the regime where the charging energy E_C is large compared to the tunnel energies J_l and J_r . We describe the dynamics in the basis of eigenstates of charge on the island, and restrict the Hilbert space to the states $|0\rangle$ and $|1\rangle$ with no and one excess Cooper pair on the island, respectively. In this two-level approximation, the Hamiltonian is given in matrix form by¹

$$\mathcal{H} = \begin{pmatrix} E_C(\frac{1}{2} + \delta n_g)^2 & J_+ \cos \frac{\varphi}{2} + iJ_- \sin \frac{\varphi}{2} \\ J_+ \cos \frac{\varphi}{2} - iJ_- \sin \frac{\varphi}{2} & E_C(\frac{1}{2} - \delta n_g)^2 \end{pmatrix} \quad (1)$$

where $J_{\pm} = \frac{1}{2}(J_l \pm J_r)$, and $\delta n_g = n_g - \frac{1}{2}$ the offset between the gate charge and the degeneracy point. Following Ref. 23, we further introduce the following quantities:

$$E_{12} = \frac{1}{2} \sqrt{J_l^2 + J_r^2 + 2J_l J_r \cos \varphi}, \quad (2a)$$

$$\gamma = \arctan \left(\frac{J_r - J_l}{J_r + J_l} \tan \frac{\varphi}{2} \right), \quad (2b)$$

$$\eta = \frac{\delta n_g}{\sqrt{\delta n_g^2 + \left(\frac{E_{12}}{E_C} \right)^2}}. \quad (2c)$$

As we are operating the pump adiabatically, we will study the dynamics in the adiabatic basis consisting of

instantaneous energy eigenstates. They are given by

$$|g\rangle = \frac{1}{\sqrt{2}} \left(\sqrt{1-\eta} |0\rangle + e^{-i\gamma} \sqrt{1+\eta} |1\rangle \right), \quad (3a)$$

$$|e\rangle = \frac{1}{\sqrt{2}} \left(\sqrt{1+\eta} |0\rangle - e^{-i\gamma} \sqrt{1-\eta} |1\rangle \right). \quad (3b)$$

In order to properly account for the pumped charge, it is essential to consider the corrections to the instantaneous ground state introduced by the time dependence of the Hamiltonian (1). These corrections can be treated perturbatively^{14,23}. For our purpose, it is sufficient to retain the first-order correction, which gives for the density operator of the sluice:

$$\rho_{gg} = 1, \quad (4a)$$

$$\rho_{ge} = \frac{i\partial_t \eta - (1-\eta^2) \partial_t \gamma}{4E_{12}}. \quad (4b)$$

We now turn to the calculation of the pumped charge. The current operator for the k -th SQUID (we set $2e = 1$ henceforth) is formally given by $\hat{I}_k = \frac{i}{\hbar} \partial_{\varphi_k} \hat{H}$, where φ_k is the phase difference across the k -th SQUID. Explicitly, one finds in the $\{|0\rangle, |1\rangle\}$ basis:

$$I_l = \frac{J_l}{2i} \begin{pmatrix} 0 & -e^{-i\varphi/2} \\ e^{i\varphi/2} & 0 \end{pmatrix} \quad (5)$$

$$I_r = \frac{J_r}{2i} \begin{pmatrix} 0 & e^{i\varphi/2} \\ -e^{-i\varphi/2} & 0 \end{pmatrix} \quad (6)$$

The expectation value of the current is given by: $I_k \equiv \text{Tr}(\hat{\rho} \hat{I}_k) = I_{d,k} + I_{p,k}$, where we have singled out a dynamic contribution $I_{d,k} = \rho_{gg} \langle g | I_k | g \rangle + \rho_{ee} \langle e | I_k | e \rangle$, and a geometric contribution $I_{p,k} = 2\Re(\rho_{ge} \langle e | I_k | g \rangle)$. The dynamic contribution is readily identified with the supercurrent leaking through the SQUIDs in the presence of a phase bias. By contrast, the geometric contribution is purely due to the pumping cycle.

The charge transferred through the k -th SQUID in a period is given by $Q_{\text{tr},k} = \int_0^T I_k(t) dt$. For adiabatic evolution, charge conservation implies $Q_{\text{tr},l} = Q_{\text{tr},r} \equiv Q_{\text{tr}}$. In light of the above discussion, it is possible to define a dynamic charge Q_d and a geometric (pumped) charge Q_p so that $Q_{\text{tr}} = Q_d + Q_p$. As shown in Ref. 3, Q_d and Q_p are related to the derivative with respect to φ of the dynamic phase Θ_d and the geometric (Berry) phase Θ_B , accumulated by the instantaneous ground state along a pumping cycle. One has, respectively:

$$Q_d = \frac{\partial \Theta_d}{\partial \varphi}, \quad (7)$$

$$Q_p = \frac{\partial \Theta_B}{\partial \varphi}. \quad (8)$$

Experimentally, Q_d and Q_p can be distinguished as they obey different symmetries. In particular upon reversing the direction of the pumping, Q_d is not affected, while Q_p duly changes its sign. We shall henceforth assume that such a distinction can be made and only be concerned with Q_p .

III. PUMPING WITH FLUXES

The principle of flux pumping is illustrated in Fig. 1 (b), showing the time evolution of the control parameters during a pumping cycle. The charge offset δn_g (not shown) is adjusted close to the degeneracy point and kept fixed throughout the cycle. At the initial time $t = 0$, the island and the leads are decoupled, with both J_l and J_r set to their minimum value J_{\min} . In sector I ($0 \leq t < T/3$), the coupling to the left lead is turned on by maximizing J_l . In sector II ($T/3 \leq t < 2T/3$), the coupling is swapped from the left to the right lead, in such a way that the sum $J_l + J_r$ is kept constant. Finally, in sector III ($2T/3 \leq t < T$) J_r is turned down to J_{\min} , bringing the system back to the initial state.

This mechanism is reminiscent of the Cooper-pair shuttle^{2,5}, as both devices rely on the maintenance of a quantum superposition of different charge states. There are, however, two fundamental differences between the Cooper-pair shuttle and the flux pump we propose. First, the movable grain acting as the “shuttle” is coupled only to one lead at a time, while in our case simultaneous coupling of the island to both leads is essential to achieve a nonvanishing pumped charge. Second, the operation of the shuttle relies on accurate control of the contact time between shuttle and leads and also of the dynamical phases accumulated by the wavefunctions along each “trip” of the shuttle. By contrast, the charge pumped by the flux pump does not depend on the speed at which the cycle is performed, as long the adiabatic theorem is obeyed. This is a consequence of the geometrical nature of the pumped charge.

In the following, we shall analyze how the pumping cycle of Fig. 1(b) determines the adiabatic dynamics of the pump, and hence the pumped charge. We first discuss the case $\varphi = 0$, as it allows for an intuitive explanation. For simplicity in deriving analytical expressions, we also set $J_{\min} = 0$.

A. The case $\varphi = 0$

At $t = 0$, the island is in a defined charge state (0 if $\delta n_g < 0$, 1 if $\delta n_g > 0$), and the energy difference between charge states is $2E_C\delta n_g$. As J_l increases so that $J_l \approx E_C\delta n_g$, the ground state evolves into a superposition of charge states. As the drive is adiabatic, charge flows from the left lead onto the island in order for the system to stay in the instantaneous ground state. The charge transferred in this case is simply given by $|\langle 1|g(\frac{T}{3})\rangle|^2 - |\langle 1|g(0)\rangle|^2$. In sector II, the swapping of the couplings does not change the Hamiltonian (1). As a result, the ground state of the island does not change and no charge is transferred. Finally, in sector III, the same amount of charge is released to the right lead, as the system has to come back (up to a geometric phase) to the initial state.

The total pumped charge for the case $\varphi = 0$ can be inferred from this heuristic argument, calculated by direct

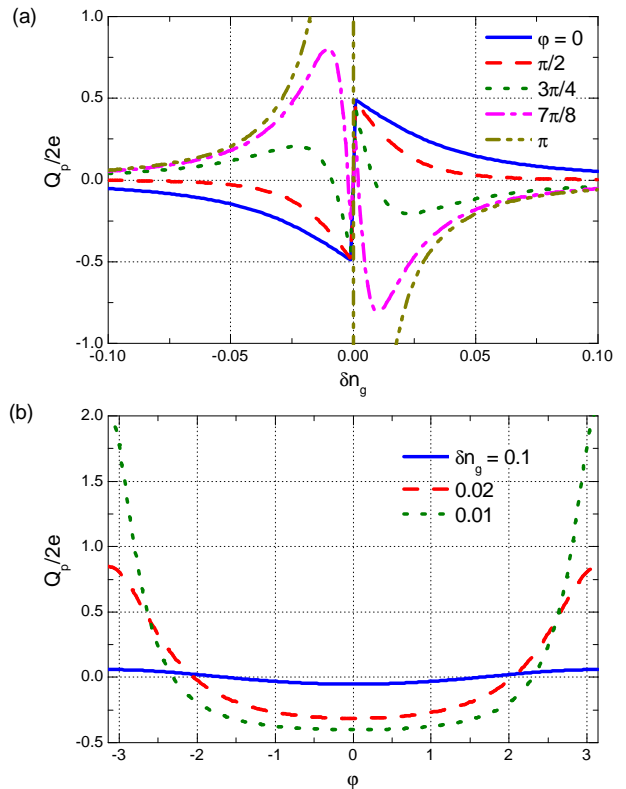


FIG. 2. (Color online) Pumped charge in the adiabatic limit. (a) Pumped charge Q_p versus offset charge δn_g for different values of the superconducting phase bias φ . (b) Q_p versus φ for different values of δn_g .

integration of $I_{p,k}$ [see Sec. II], or obtained by virtue of (8) [see Appendix A]. In each case, the result is:

$$Q_p[\varphi = 0] = -\frac{1}{2}\text{sgn}(\delta n_g) \left(1 - \frac{1}{\sqrt{1+r^2}} \right), \quad (9)$$

where we have introduced the ratio

$$r = \frac{J_{\max}}{2E_C\delta n_g}. \quad (10)$$

In the limit $r \rightarrow \pm\infty$ (corresponding to $E_C|\delta n_g| \ll J_{\max}$), the absolute value of Q_p approaches a maximum of half a Cooper pair. This result is approximately valid also for a finite J_{\min} , as long as $J_{\min} \ll E_C\delta n_g$.

The dependence of Q_p on δn_g exhibits a sawtooth behavior, as shown by the solid line in Fig. 2(a). At $\delta n_g = 0$, the pumped charge changes sign discontinuously. However, when $\delta n_g \rightarrow 0$ also the minimum energy gap $\Delta E_{\min} \equiv \min_{t \in [0, T]} \Delta E(t) = \delta n_g E_C$ tends to zero. This implies that the adiabatic limit, in which the present derivation is valid, is only attained for infinitely slow evolution. We will return to this point in Sec. IV.

B. The general case

When $\varphi \neq 0$, the same calculation leading to (9) shows that the pumped charge in sectors I and III is the same as in the case $\varphi = 0$. This is only to be expected: as long as the island is only coupled to a single lead, the phase difference between the leads cannot play any role. The situation is different for sector II, where the coupling swap now takes place between two leads at different phases. As a result, an adjustment of the superconducting order parameter on the island is required.²⁵ This causes an additional geometric current to flow across the sluice, in a direction opposite to that of the pumping.

In Fig. 2(a) we plot Q_p versus δn_g for different values of φ . For values of φ in the range of 0 and $\pi/2$, Q_p simply decreases with respect to the case $\varphi = 0$. As φ is further increased, however, a new trend emerges: Q_p changes its sign with respect to the unbiased case, except in the vicinity of the degeneracy point. The magnitude of the counterflowing Q_p can well exceed a Cooper pair. Finally, at $\varphi = \pi$ the sign of the pumped charge is opposite to that of the unbiased case for all values of δn_g . Furthermore, Q_p diverges as $1/\delta n_g$ for $\delta n_g \rightarrow 0$.

The full dependence of Q_p on φ is shown in Fig. 2(b) for three selected values of δn_g . The reader may guess that the integral of each curve in Fig. 2(a) vanishes. Indeed, using (8) we obtain $\langle Q_p \rangle_\varphi \equiv \frac{1}{2\pi} \int_0^{2\pi} Q_p(\varphi) d\varphi = \Theta_B(2\pi) - \Theta_B(0)$. While for the Cooper-pair sluice $\Theta_B = \varphi + \epsilon \sin \varphi$ (ϵ is a small correction),⁶ so that $\langle Q_p \rangle_\varphi = 1$, in our case $\Theta_B(2\pi) = \Theta_B(0)$, so that $\langle Q_p \rangle_\varphi = 0$. This implies that flux pumping can only be observed in the presence of a well-defined phase bias, for if φ randomly oscillates in time, then no net charge is transferred on average. On the other hand, Q_p exhibits some degree of robustness against small phase fluctuations. In particular, for $\delta n_g \ll 1$, Q_p develops a plateau centered at $\varphi = 0$. This can be seen in the increased flattening of the curves with smaller δn_g in Fig. 2(b) (an analytical argument is provided in the Appendix).

We shall now fix our attention on the case $\varphi = \pi$, for which we can present analytical results. Upon direct integration of the current operator, we obtain for the charge pumped in the sector II

$$Q_p^{(\text{II})}[\varphi = \pi] = \text{sgn}(\delta n_g) \frac{r^2}{2\sqrt{1+r^2}}. \quad (11)$$

This must be added to the contribution (9) from sectors I,III, to give the total pumped charge

$$Q_p[\varphi = \pi] = \frac{1}{2} \text{sgn}(\delta n_g) \left(\sqrt{1+r^2} - 1 \right). \quad (12)$$

An alternative derivation of (12) involving the Berry phase is shown in Appendix A. On comparing (9) and (12), we see that the pumping direction for $\varphi = \pi$ is always opposite to that for $\varphi = 0$. From (12), it is apparent that Q_p diverges for $\varphi = \pi$ and $r \rightarrow \infty$ (or $\delta n_g \rightarrow 0$).

Notably, one finds that this divergence is not removed even when relaxing the constraint $J_{\min} = 0$.

The present results are supposed to hold in the adiabatic limit, which requires $|\rho_{ge}| \ll 1$. For $\varphi = \pi$, $|\rho_{ge}|$ is maximum at $t = T/2$, where it attains the value

$$\max_{0 \leq t < T} |\rho_{ge}| = \frac{3\hbar r^2}{J_{\max} T}. \quad (13)$$

We thus see that $|\rho_{ge}|$ also diverges for $r \rightarrow \infty$. This implies that when approaching the degeneracy point, the pumping period should be increased according to $T \propto r^2$ in order to stay in the adiabatic limit. In other words, the increase in Q_p comes at the cost of an increasingly long T . One can further check that the pumping current I_p does not diverge at any time. In fact, I_p never exceeds $I_{\max} \approx \frac{J_{\max}}{4\hbar} \rho_{ge} \ll \frac{J_{\max}}{\hbar}$, that is, much less than the critical current of the SQUIDs.

IV. ADIABATIC BREAKDOWN AND DECOHERENCE

In Sec. III, we carried out our calculations assuming adiabatic evolution during the pumping cycle. In this limit, the pumped charge is a property of the loop described in the parameter space of the Hamiltonian (1). As such, it does not depend on the pumping frequency. We also pointed out, however, that the validity of the adiabatic theorem requires the condition $|\rho_{ge}| \ll 1$ to hold. We then warned the reader that in the limit $\delta n_g \rightarrow 0$, due to the vanishing of the instantaneous energy gap at $t = 0$ (and at $t = T/2$ when $\varphi = \pi$), this condition requires the pumping cycle to be infinitely slow. As real measurements are always performed at finite frequencies, this implies that none of the traces of Fig. 2(a) can be exactly reproduced in an experiment in the vicinity of $\delta n_g = 0$.

In this Section, we investigate how the breakdown of the adiabatic limit affects the pumped charge. As soon as we allow nonadiabatic transitions to take place, the dynamics of the system becomes highly nontrivial. As argued elsewhere^{12,14,22,23}, the pumped charge is a sensitive probe of this dynamics. Indeed, it was exploited in Ref. 19 to characterize Landau-Zener transitions in the Cooper-pair sluice. Furthermore, the final state of the pump at the end of the pumping cycle is in general different from its initial state. As measurements are typically averaged over very many cycles, the quantity of experimental interest becomes the stationary pumped charge Q_p^{st} ,²⁴ determined by the interplay between the nonadiabatic drive and the electromagnetic environment in which the pump is embedded.

The numerical results we present are obtained using the Master-Equation approach developed in Refs. 22 and 23, which consistently accounts for the combined action of a quasi-adiabatic drive and decoherence on an open quantum two-level system. This formalism is not intended to address the fully nonadiabatic case; yet, it can

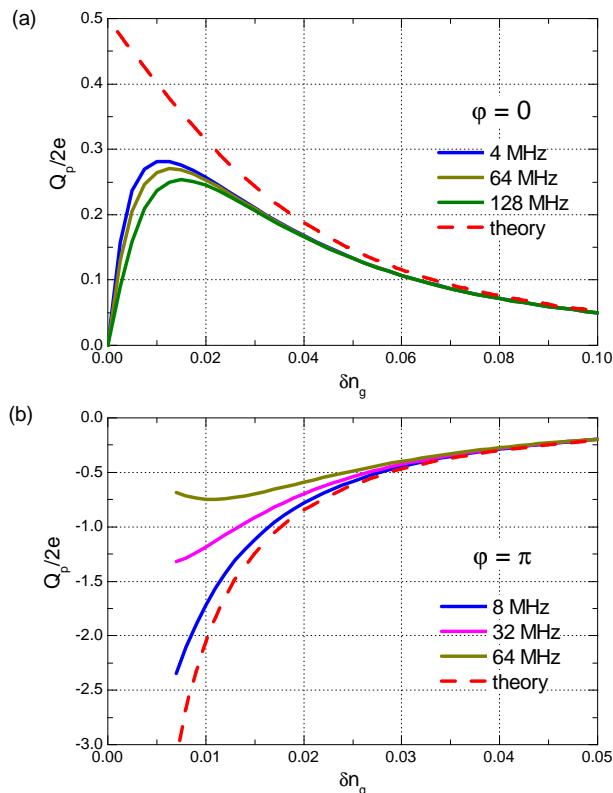


FIG. 3. (Color online) Breakdown of the adiabatic limit. Q_p versus δn_g for $\varphi = 0$ (a) and $\varphi = \pi$ (b), for different pumping frequencies f (solid lines). The results are obtained by numerical integration of the Master Equation of Ref. 22. The asymptotic (adiabatic-limit) Q_p , calculated according to (9) and (12), is also shown for comparison (dashed lines). Relevant parameter values for the pump are: $E_C = 1$ K, $J_{\max} = 0.1E_C$, $J_{\min} = 0.03J_{\max}$. For the fictitious environment (see Ref. 23 for details): $g = 0.02$, $R = 300$ k Ω , $T = 0$, $T_0 = 0.4$ K.

be conveniently used to investigate the parameter region where the adiabatic limit breaks down. Decoherence (dephasing and relaxation) is modeled by attaching a fictitious environment to the pump, in the form of a resistor capacitively coupled to the central island. This mimics the effect of charge noise, which is known to be the first cause of decoherence in charge-based devices²⁶.

A full characterization of the effects of decoherence on flux pumping is beyond the scope of this work. Still, including decoherence in the model is essential in order to reach a quasistationary state. In the following, we will consider a zero-temperature environment and set the coupling parameter to a value small enough that the effects of nonadiabatic transitions are not washed out by environment-induced relaxation²².

In Fig. 3 we plot Q_p^{st} versus δn_g for the emblematic cases $\varphi = 0$ (a) and $\varphi = \pi$ (b). We choose the realistic device parameters $E_C = 1$ K, $J_{\max} = 0.1E_C$, $J_{\min} = 0.03J_{\max}$, and explore different pumping frequencies (solid lines). The adiabatic-limit predictions for the two

cases (Eqs. 9 and 12, respectively) are also plotted for comparison (dashed lines); notice, however, that they were derived in the limit $J_{\min} \rightarrow 0$.

In general, nonadiabatic transitions result in a decrease of Q_p . This is qualitatively accounted for by the fact that the adiabatic excited state of the sluice carries an opposite Q_p with respect to the ground state. For the case $\varphi = 0$ [Fig. 3(a)], this results in a smearing of the adiabatic sawtooth. Note that since we have considered the realistic case $J_{\min} \neq 0$, in the limit $\delta n_g \rightarrow 0$ one still has $\Delta E_{\min} = J_{\min}$, so that the residual coupling partly holds back nonadiabatic transitions. Analogous considerations can be made for the case $\varphi = \pi$ [Fig. 3(b)]. As δn_g is reduced, however, the nonadiabatic behavior is no longer mitigated by the presence of a finite J_{\min} (this relates to the fact that E_{12} vanishes for $J_l = J_m$ when $\varphi = \pi$, see Eq. 2a). The effect is thus more dramatic, with higher frequencies hitting the nonadiabatic onset first. We are not running the simulation for parameter values too close to $\delta n_g = 0$, as they fall outside the range of validity of our Master Equation.

V. CONCLUSIONS

We have presented a scheme for Cooper-pair pumping which uses neither a bias voltage nor a modulation of gate voltages. This scheme involves the adiabatic and coherent transfer of a superposition of charge states across a superconducting island. It requires a definite phase bias to work properly, and presents a peculiar dependence on this bias. In particular, when the phase bias is π , the pumped charge per cycle can become arbitrarily large near the gate degeneracy point. The pumped current, however, is bounded by the adiabaticity criterion, which dictates that in the same regime the pumping frequency has to be correspondingly small.

The realization of this scheme looks feasible, especially in light of recent results obtained with the Cooper-pair sluice^{17,19}. To this end, particular care must be taken in controlling the phase bias. This can be achieved, e. g., by embedding the pump in a fully superconducting loop together with a large Josephson junction. In this configuration, the latter would also serve as a current threshold detector, as in Ref. 17.

An apparent matter of concern is the fact that at finite phase, the supercurrent leaking through the device may well exceed the pumped current. For instance, let us take the device parameters of Fig. 3 and the pumping cycle of Fig. 1(a). The mean dynamic current at $\varphi = \pi/2$ can be approximated by $I_d \approx \frac{2e}{24\hbar} J_{\max} \approx 350$ pA, independent of frequency. This is to be compared to the pumping current $I_p = Q_p f$. At a typical $f = 120$ MHz, $Q_p = e$ corresponds to $I_p \approx 20$ pA, so that the pumped current accounts for less than 10% of the signal. This is not an issue, however, as the supercurrent term is even with respect to time-reversal symmetry, while the pumped current is odd. As a result, we can determine I_p by simply

subtracting the measured currents when pumping in opposite directions (as done in Ref. 17).

Still, detecting such a small current circulating in a loop may challenge customary techniques. In the search for signatures of flux pumping, an important role is likely to be played by its distinctive symmetries. Besides time-reversal, I_p is also an odd function of the gate position with respect to degeneracy. Finally, it should not depend on the direction of the circulating currents in the SQUIDs. Altogether, these symmetries may be used to rule out the contribution of undesired rectification effects, possibly originating from spurious inductive or capacitive couplings.

ACKNOWLEDGMENTS

The authors are grateful to T. Aref, L. Arrachea, F. Gizotto, J. Pekola, A. Shnirman, and P. Solinas for valuable discussions. This work was supported by the European Community FP7 under grant No. 238345 “GE-OMDISS”. S. G. acknowledges financial support from the Finnish National Graduate School in Nanoscience.

Appendix A: Flux pumping and Berry phase

The charge pumped by a superconducting pump in the adiabatic limit is linked to the Berry phase Θ_B accumulated by the instantaneous ground state along the pumping cycle³, as prescribed by (8). For a two-level system parametrically driven in closed loop, Θ_B is proportional to the solid angle spanned by the Bloch vector, which performs an adiabatic rotation on the Bloch sphere. The path drawn by the Bloch vector is shown in Fig. 4(a) for the pumping cycle of Fig. 1(b) and a few selected values of φ . The resulting Θ_B is plotted versus φ and δn_g in Fig. 4(b). According to (8), the pumped charge Q_p is given by the local slope of the surface plot along the φ axis.

Using (2), (3), and the definition²⁰, we find

$$\Theta_B \equiv i \int_0^T dt \langle g | \dot{g} \rangle = \frac{1}{2} \int_0^T dt (1 + \eta) \dot{\gamma}. \quad (\text{A1})$$

For the given pumping cycle, $\gamma(t) = -\varphi/2$ in sector I and $\gamma(t) = \varphi/2$ in sector III. The time derivative of γ vanishes in these regions. The sudden change of γ from $\varphi/2$ to $-\varphi/2$ at times $0, T, \dots$ yields a delta function in the time derivative, but at that time $1 + \eta = 0$, so that the integrand in (A1) vanishes as well. As a result, the only contribution to Θ_B comes from sector II. The fact that sectors I and III do not contribute to Θ_B is a consequence of our choice of adiabatic basis (Eqs. 3), and is not in contrast with the fact that there is a charge flow in sectors I, III. Indeed, Θ_B is only defined for closed loops. It is possible to give a gauge-invariant generalization of the Berry phase for open loops²⁷, but we will not need it here.

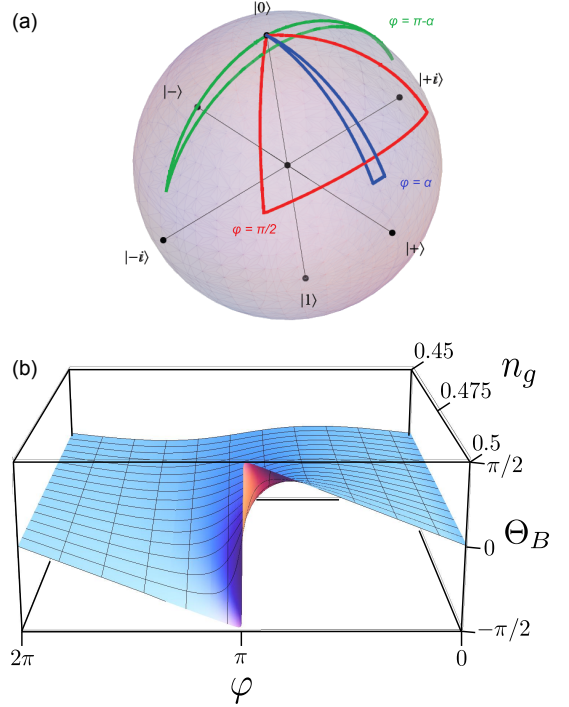


FIG. 4. (Color online) (a) Plots of the path drawn by the ground state of the sluice on the Bloch sphere along a pumping cycle, for $\varphi = \alpha$ (blue), $\varphi = \pi/2$ (red), and $\varphi = \pi - \alpha$ (green), with $\alpha \ll 1$. The Berry phase is proportional to the solid angle spanned by the paths. (b) Berry phase Θ_B versus φ and δn_g . According to (8), The pumped charge Q_p is proportional to the slope of the surface plot along the φ axis.

We will now explicitly calculate Θ_B and Q_p in two important cases.

1. Case $\varphi = 0$

For definiteness, we assume $\delta n_g < 0$. To calculate Q_p for $\varphi = 0$, it is sufficient to expand Θ_B to first order in φ . Up to this order, η is time-independent in sector II, so that $\Theta_B \approx \frac{1}{2}(1 + \eta)[\gamma(2T/3) - \gamma(T/3)] = \frac{1}{2}(1 + \eta)\varphi$. The pumped charge is thus

$$Q_p[\varphi = 0] = \frac{1}{2}(1 - \eta), \quad (\text{A2})$$

as we found in (9).

It is worth noting that near the degeneracy point $\delta n_g \ll 1$, the validity of (A2) extends to all phases $\varphi \neq \pi$. In fact, for sufficiently small δn_g , $\eta \approx 0$ for all times in sector II. As a result, the pumped charge is half a Cooper pair, as predicted by (A2).

2. Case $\varphi = \pi$

to give

Using (8) and (A1), we find for the pumped charge

$$Q_P[\varphi = \pi] = \frac{1}{2} \int_{T/3}^{2T/3} dt \left[1 + \frac{\delta n_g}{\sqrt{\delta n_g^2 + [(J_l - J_r)/(2E_C)]^2}} \right] \times \frac{\partial^2}{\partial t \partial \varphi} \arctan \left(\frac{J_r - J_l}{J_r + J_l} \tan \frac{\varphi}{2} \right). \quad (\text{A3})$$

$$Q_P[\varphi = \pi] = \frac{T}{12} \int_0^{T/6} \frac{du}{u^2} \left[1 - \frac{1}{\sqrt{1 + (6ru/T)^2}} \right] = \frac{1}{2} \left[\sqrt{1 + r^2} - 1 \right]. \quad (\text{A4})$$

Using $J_r + J_l = J_{\max}$ and $J_r - J_l = 6J_{\max}u/T$ with $u = t - T/2$, the integral can be evaluated analytically

- ¹ J. P. Pekola, J. J. Toppari, M. Aunola, M. T. Savolainen, and D. V. Averin, Phys. Rev. B, **60**, R9931 (1999).
- ² L. Y. Gorelik, A. Isacsson, Y. M. Galperin, R. I. Shekhter, and M. Jonson, Nature, **411**, 454 (2001).
- ³ M. Aunola and J. J. Toppari, Phys. Rev. B, **68**, 020502(R) (2003).
- ⁴ A. O. Niskanen, J. P. Pekola, and H. Seppä, Phys. Rev. Lett., **91**, 177003 (2003).
- ⁵ A. Romito, F. Plastina, and R. Fazio, Phys. Rev. B, **68**, 140502 (2003).
- ⁶ M. Möttönen, J. P. Pekola, J. J. Vartiainen, V. Brosco, and F. W. J. Hekking, Phys. Rev. B, **73**, 214523 (2006).
- ⁷ M. Cholasinski and R. W. Chhajlany, Phys. Rev. Lett., **98**, 127001 (2007).
- ⁸ S. Safaei, S. Montangero, F. Taddei, and R. Fazio, Phys. Rev. B, **77**, 144522 (2008).
- ⁹ R. Leone, L. P. Lévy, and P. Lafarge, Phys. Rev. Lett., **100**, 117001 (2008).
- ¹⁰ V. Brosco, R. Fazio, F. W. J. Hekking, and A. Joye, Phys. Rev. Lett., **100**, 027002 (2008).
- ¹¹ J.-M. Pirkkalainen, P. Solinas, J. P. Pekola, and M. Möttönen, Phys. Rev. B, **81**, 174506 (2010).
- ¹² S. Gasparinetti, P. Solinas, and J. P. Pekola, Phys. Rev. Lett., **107**, 207002 (2011).
- ¹³ I. Kamleitner and A. Shnirman, Phys. Rev. B, **84**, 235140 (2011).
- ¹⁴ J. Salmilehto and M. Möttönen, Phys. Rev. B, **84**, 174507 (2011).
- ¹⁵ L. J. Geerligs, S. M. Verbrugh, J. E. Mooij, H. Pothier, C. Urbina, and M. H. Devoret, Z. Phys. B, **85**, 349 (1991).
- ¹⁶ A. O. Niskanen, J. M. Kivioja, H. Seppä, and J. P. Pekola, Phys. Rev. B, **71**, 012513 (2005).
- ¹⁷ M. Möttönen, J. J. Vartiainen, and J. P. Pekola, Phys. Rev. Lett., **100**, 177201 (2008).
- ¹⁸ F. Hoehne, Y. A. Pashkin, O. V. Astafiev, M. Möttönen, J. P. Pekola, and J. S. Tsai, Phys. Rev. B, **85**, 140504 (2012).
- ¹⁹ S. Gasparinetti, P. Solinas, Y. Yoon, and J. P. Pekola, Phys. Rev. B, **86**, 060502(R) (2012).
- ²⁰ M. V. Berry, Proc. R. Soc. Lond. A, **392**, 45 (1984).
- ²¹ B. Simon, Phys. Rev. Lett., **51**, 2167 (1983).
- ²² J. P. Pekola, V. Brosco, M. Möttönen, P. Solinas, and A. Shnirman, Phys. Rev. Lett., **105**, 030401 (2010).
- ²³ P. Solinas, M. Möttönen, J. Salmilehto, and J. P. Pekola, Phys. Rev. B, **82**, 134517 (2010).
- ²⁴ A. Russomanno, S. Pugnetti, V. Brosco, and R. Fazio, Phys. Rev. B, **83**, 214508 (2011).
- ²⁵ This can be seen by introducing the operator $e^{i\hat{\theta}}$, related to the charge number operator \hat{N} by the commutation rule $[\hat{N}, e^{i\hat{\theta}}] = e^{i\hat{\theta}}$. Its representation in the reduced charge basis is given by $e^{i\hat{\theta}} = |1\rangle\langle 0|$. Using (3), one can show that $\langle g|e^{i\hat{\theta}}|g\rangle = e^{i\gamma}$. We thus identify γ with the expectation value of the phase of the island. As expected, γ equals the phase of the left lead at the beginning of sector II, and that of the right lead at its end.
- ²⁶ G. Ithier, E. Collin, P. Joyez, P. J. Meeson, D. Vion, D. Esteve, F. Chiarello, A. Shnirman, Y. Makhlin, J. Schrieffer, and G. Schön, Phys. Rev. B, **72**, 134519 (2005).
- ²⁷ J. Samuel and R. Bhandari, Phys. Rev. Lett., **60**, 2339 (1988).